

# Optimal Aggregation of RF and VLC Bands for Beyond 5G Mobile Services

Dimitrios Bozanis\*, Vasilis K. Papanikolaou\*, Alexis A. Dowhuszko<sup>†</sup>, Konstantinos G. Rallis\*, Panagiotis D. Diamantoulakis\*, Jyri Hämäläinen<sup>†</sup>, and George K. Karagiannidis\*

\*Department of Electrical and Computer Engineering, Aristotle University of Thessaloniki, GR-54124 Thessaloniki, Greece

<sup>†</sup>Department of Communications and Networking, Aalto University, 02150 Espoo, Finland

Emails: dimiboz@ece.auth.gr, vpapanikk@auth.gr, alexis.dowhuszko@aalto.fi, konralgeo@ece.auth.gr, padiaman@ieee.org, jyri.hamalainen@aalto.fi, geokarag@auth.gr

**Abstract**—The integration of Radio Frequency (RF) and Visible Light Communication (VLC) technologies has been considered an enabler to achieving the Key Performance Indicators (KPIs) in Beyond 5G (B5G). Apart from higher data rates for enhanced Mobile Broadband applications, Ultra-Reliable and Low-Latency Communications and massive Machine-Type Communications must be also supported. This poses notable challenges in the design of a mobile communication system that relies exclusively on the use of licensed RF spectrum. In order to cope with the requirements of B5G services, the complementary benefits that RF and VLC bands have in terms of communication bandwidth, signal propagation characteristics, and ultra-densification feasibility, can be exploited. For this purpose, this paper studies the performance of two integration approaches, namely RF-VLC selection (Layer-3 or network-layer) and RF-VLC aggregation (Layer-2 or MAC-layer). Based on the obtained simulation results, it is possible to conclude that RF-VLC aggregation outperforms RF-VLC selection in terms of data rate performance, especially when ultra-reliable communication services are required to connect a large number of user terminals placed in an indoor scenario.

**Index Terms**—Hybrid RF-VLC systems, Carrier Aggregation, RAT Selection, Visible Light Communication, Resource Allocation, Ultra-Reliable Communications, New Radio, B5G.

## I. INTRODUCTION

The Fifth Generation (5G) of mobile networks, which relies on very dense networking, has started to be deployed in major urban centers all over the globe. With the aid of novel technologies such as Millimetre Wave (MMW) and Software-Defined Network (SDN), as well as the evolution of the ones existing in 4G, 5G can provide new kinds of services, which are known as enhanced Mobile Broadband (eMBB), Ultra-Reliable Low-Latency Communications (URLLC), and massive Machine-Type Communications (mMTC) [1], [2]. Though contemporary (4G/5G) mobile networks rely on communications over (licensed) Radio Frequency (RF) bands, the integration of Optical and RF wireless technologies have the potential to provide notable gains in Beyond 5G (B5G) scenarios, especially in indoor environments.

Visible light communication (VLC) is an optical wireless technology that has lately emerged as a novel solution to prevent the RF spectrum shortage that is foreseen in B5G [3]. VLC uses the much larger bandwidth that is available in the optical portion of the electromagnetic spectrum, which

is license-free by definition and takes advantage of the fast time response of Light-Emitting Diodes (LEDs) and Photodiodes (PDs) to transmit wideband data-carrying signals. Multi-cell VLC systems have been considered to provide indoor wireless coverage by reusing existing LED light fixtures to enable communication services on top of illumination [4]. Different approaches have been considered in the literature to mitigate the strong inter-cell interference that emerges in ultra-dense VLC small cell deployments [5], [6]. Nevertheless, most of these publications consider that the multi-cell VLC system is stand-alone by default and, in those cases where RF-VLC integration is considered, it is assumed to happen at the wireless access technology level by selecting to use either RF or VLC to serve the target terminal (RF-VLC selection) [7].

When using *RF-VLC selection* as an integration approach in hybrid RF-VLC networks, each user terminal should have open data links simultaneous over RF and VLC data carriers; then, the most convenient wireless access technology should be selected to route data packets over a tunnel at the Network layer (L3). For this purpose, VLC access points should be deployed to provide full coverage in the target service area, which is a demanding task when dealing with irregular floor plans [8]. Moreover, strong inter-cell interference will happen in this situation in VLC cell-edge areas, affecting the achievable data rate when a unitary frequency reuse factor is used [9]. In contrast, when using *RF-VLC aggregation*, data traffic splits between RF and VLC carriers at the MAC layer. This way, scheduling decisions could be made at the transmission time interval level (per communication frame), reacting much faster to changes and enabling the reception of information from both RF and VLC carriers simultaneously.

This paper studies the performance of both integration approaches, *i.e.*, RF-VLC selection and RF-VLC aggregation, when the aim is to improve the mean data rate (and reliability) of a single-cell 5G system. The proposed mobile system architecture is similar to the Coordinated-Multi Point transmission scenarios for downlink presented in [10], but replaces the 4G macro-cell with a 5G small cell on licensed RF spectrum, and the Remote Radio Units (RRUs) with Remote Optical Units (ROUs) on unlicensed optical spectrum. Due to that, the optimization problem to be solved resembles the one presented in [11] in terms of orthogonal resource allocation per cell,

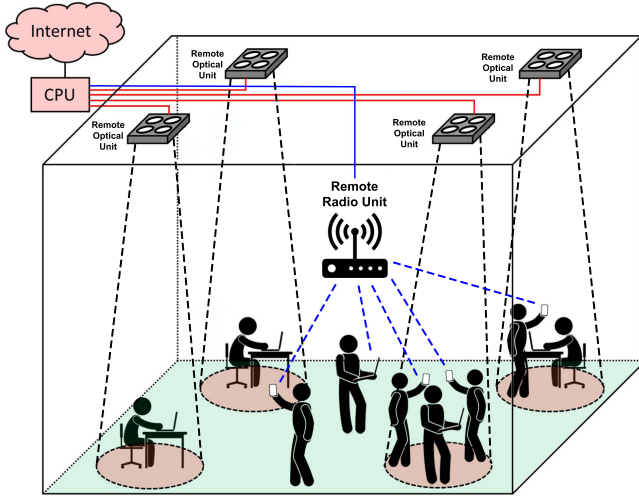


Fig. 1: The proposed hybrid RF-VLC system.

replacing the RF channels models with optical wireless ones for the VLC cells, adding an RF layer that can provide wireless coverage in the whole room, and replacing the distributed resource allocation approach for a centralized one [9]. Notable performance gains are observed when both VLC and RF carriers are jointly used to serve the users that are randomly deployed in the room. This gain is observed not only in the median data rate of the mobile users which is valid for eMBB, but also in the outage capacity that is relevant for URLLC.

## II. SYSTEM MODEL

Let us consider the indoor downlink transmission scenario illustrated in Fig. 1, in which mobile users with index  $n$  in set  $\mathcal{N} = 1, \dots, N$  have the possibility to receive data over RF (dashed blue lines) and VLC (red spots) wireless links on different parts of the room. Similarly, let us assume that  $i$  in set  $\mathcal{I} = 1, \dots, I$  and  $j$  in set  $\mathcal{J} = 1, \dots, J$  are the indexes of the RRUs and ROUs, respectively. It is also considered that interference between the same kind of Remote Units (RUs) may take place when their cell coverage areas overlap

In this situation, the aggregate data rate that a target mobile user with index  $n$  can achieve is given by

$$R_n = \sum_{i \in \mathcal{I}} \alpha_{i,n} r_{i,n}^{(\text{RF})} + \sum_{j \in \mathcal{J}} \beta_{j,n} r_{j,n}^{(\text{VLC})}, \quad (1)$$

where  $r_{i,n}^{(\text{RF})}$  and  $r_{j,n}^{(\text{VLC})}$  are the achievable data rates when all the communication resources in RRU  $i$  (RF) and ROU  $j$  (VLC) are allocated to serve user  $n$ , respectively. Similarly,  $\alpha_{i,n}, \beta_{j,n} \in [0, 1]$  are the scheduling weights, or equivalently the fraction of the orthogonal communication resources that RRU  $i$  and RRO  $j$  reserve to serve user  $n$ , respectively.

Four different transmission schemes are studied in this paper, which differentiates from each other as follows:

- 1) For *RF-only*,  $\beta_{j,n} = 0$  for all  $j \in \mathcal{J}$  and  $n \in \mathcal{N}$ . Moreover we assume that each user is served by one

RRU and that the communication resources excess is constrained by  $\sum_{n \in \mathcal{N}} \alpha_{i,n} \leq 1$  for all  $i \in \mathcal{I}$ .

- 2) For *VLC-only*,  $\alpha_{i,n} = 0$  for all  $i \in \mathcal{I}$  and  $n \in \mathcal{N}$ . Without loss of generality, we assume that each user is served by a single ROU, verifying  $\sum_{n \in \mathcal{N}} \beta_{j,n} \leq 1$  for all  $j \in \mathcal{J}$ .
- 3) For *RF-VLC selection*, as each user is served max by one RU,  $\alpha_{i,n} \times \beta_{j,n} = 0$  is added as additional constraint for all  $i \in \mathcal{I}, j \in \mathcal{J}$ , and  $n \in \mathcal{N}$ . Note that in this situation, communication happens either over RF (RRU) or VLC (ROU), but not simultaneously over both kinds of the spectrum, with respect to the resource's constraints.
- 4) Finally, for *RF-VLC aggregation* simultaneous communication over RF and VLC is possible, verifying both the RF and VLC resource's constraints, as they were presented for *RF-only* and *VLC-only*.

We now model the data rate that each user can receive on RF and VLC bands when placed on different parts of the room.

### A. Achievable data rate for the radio access links

The path loss factor for the RF link from RRU  $i$  to mobile user  $n$  is denoted by  $L_{i,n}$ , whereas the normalized fast fading coefficient for the same RF link is given by  $g_{i,n}$ . Due to the fact that OMA (e.g., OFDMA) is assumed in the RF-based downlink, intra-cell interference is avoided; however, notable inter-cell interference may still happen, especially if more than one RRU is deployed in the same room. Thus, the Signal-to-Interference-plus-Noise power Ratio (SINR) in the RF link from RRU  $i$  to mobile user  $n$  becomes

$$\gamma_{i,n}^{(\text{RF})} = \frac{|g_{i,n}|^2 P_i / L_{i,n}}{\underbrace{\sum_{k \in \mathcal{I}; k \neq i} |g_{k,n}|^2 P_k / L_{k,n}}_{\text{Inter-cell interference power}} + \underbrace{N_0 B_i}_{\text{AWGN power}}}, \quad (2)$$

where  $P_i$  denotes the mean transmission power of RRU  $i$ ,  $B_i$  is the communication bandwidth of the same RRU, and  $N_0$  is the spectral power density of the Additive White Gaussian Noise (AWGN) in the RF system. Based on these considerations, the achievable data rate for mobile use  $n$  in the RF carrier can be estimated with the Shannon formula, i.e.,

$$r_{i,n}^{(\text{RF})} = B_i \log_2 \left( 1 + \gamma_{i,n}^{(\text{RF})} \right), \quad (3)$$

where  $B_i$  are the orthogonal communication resources that RRU  $i$  can allocate to its associated users. Finally, the RF data rate that mobile user  $n$  receives is given by

$$R_n^{(\text{RF})} = \sum_{i \in \mathcal{I}} \alpha_{i,n} r_{i,n}^{(\text{RF})} \quad n = 1, \dots, N. \quad (4)$$

We note that in this paper we assume a single RRU ( $I = 1$ ).

### B. Achievable data rate for the optical wireless access links

The optical wireless channel power gain between ROU  $j$  and mobile station  $n$  is denoted by  $h_{j,n}$ . Since the use of an OMA scheme (e.g., optical OFDMA/SC-FDMA/TDMA) generates the same effect in terms of intra- and inter-cell

interference as the one explained in Section II-A, the SINR of the optical wireless link from ROU  $j$  to mobile station  $n$  is

$$\gamma_{j,n}^{(\text{VLC})} = \frac{\left(h_{j,n} \eta p_j\right)^2}{\underbrace{\sum_{k \in \mathcal{J}; k \neq j} \left(h_{k,n} \eta p_k\right)^2}_{\text{Inter-cell interference power}} + \underbrace{\sigma_n^2 W_j}_{\text{AWGN power}}} \quad (5)$$

where  $\eta$  denotes the responsivity of the PD in the VLC receiver,  $p_j$  is the optical power that ROU  $j$  allocates for communication in transmission to transmit the data-carrying signal,  $\sigma_n^2$  is the variance of the AWGN noise in the VLC receiver, and  $W_j$  is the electrical modulation bandwidth of ROU  $j$ . Then, the achievable data rate for a mobile user with index  $n$  in the VLC carrier can be approximated with the lower bound for the capacity of an intensity-modulated direct-detected optical wireless channel [12], which is given by

$$r_{j,n}^{(\text{VLC})} = W_j \log_2 \left( 1 + \frac{e}{2\pi} \gamma_{j,n}^{(\text{VLC})} \right), \quad (6)$$

where  $W_j$  are the orthogonal communication resources that ROU  $j$  can allocate to its associated mobile users. Finally, the VLC data rate that mobile user  $n$  receives is given by

$$R_n^{(\text{VLC})} = \sum_{j \in \mathcal{J}} \beta_{j,n} r_{j,n}^{(\text{VLC})}. \quad (7)$$

Note that data rates in (4) and (7) do not necessarily imply that RF and VLC aggregation is possible, but rather show the data rate that is feasible for user  $n$  in each kind of spectrum.

### III. RESOURCE ALLOCATION

In this paper, a centralized resource manager is used to define the most convenient allocation of RF and VLC band resources, in order to achieve the target optimization goal.

#### A. Proportional fair utility function

In resource allocation problems within heterogeneous networks, different network attributes affect the Quality of Service (QoS) of the involved users. In this particular RF-VLC setting, the mobile users that do not have VLC coverage and are relatively distant from the RRUs are expected to experience low QoS, especially when many users must compete for the same (limited) communication resources that are available. In general, various fairness metrics have been introduced in the literature for similar problems, where an effective compromise between the overall sum data rate and user fairness needs to be achieved. In this work, the proportional fairness metric [13], [14] is used, being defined as the natural logarithm of the data rate  $R_n$  for mobile user  $n$ , as given in (1). That is,

$$u_n(R_n) = \ln(R_n). \quad (8)$$

Similarly, the system-level proportional fair utility function is

$$u_{\text{sum}}(R_1, \dots, R_N) = \sum_{n \in \mathcal{N}} u_n(R_n) = \sum_{n \in \mathcal{N}} \ln(R_n), \quad (9)$$

which is also an increasing function of the data rate of the users in the system. Note that since the logarithmic function

decreases very fast when its argument tends to zero, those resource allocation solutions that provide very low data rates to some mobile users will be discouraged, as they will yield significantly low values of the individual proportional fairness utility, impacting notably the sum utility for the whole system.

#### B. Formulation of the centralized optimization problem

The formulation of a Resource Allocation (RA) problem is now investigated to enable the convenient division of communications resources in both RF and VLC bands. Without loss of generality, the following analysis aims at maximizing the sum proportional fairness utility of mobile users. Moreover, because of the use of OMA schemes in both RF and VLC carriers, the allocation of communication resources for each mobile user in each RRU and ROU of the wireless system is jointly optimized. Because of the four schemes that are examined, the optimization problem differentiates, thus each case will be studied separately. Taking (1) and (9) into consideration, the objective function can be expanded as

$$\sum_{n \in \mathcal{N}} \ln(R_n) = \sum_{n \in \mathcal{N}} \ln \left( \sum_{i \in \mathcal{I}} \alpha_{i,n} r_{i,n}^{(\text{RF})} + \sum_{j \in \mathcal{J}} \beta_{j,n} r_{j,n}^{(\text{VLC})} \right). \quad (10)$$

Let  $\mathbf{A} = (\alpha_{i,n}) \in \mathbb{R}^{I \times N}$  and  $\mathbf{B} = (\beta_{j,n}) \in \mathbb{R}^{J \times N}$  denote the scheduling weights matrices for RF and VLC resources, where  $\alpha_{i*}$ ,  $\beta_{j*}$  stand for their  $i$ -th and  $j$ -th row, respectively, whereas  $\alpha_{*n}$ ,  $\beta_{*n}$  stand for their  $n$ -th column, respectively.

1) *Standalone RF-only network*: As it was explained in Section II, for a standalone RF network  $\mathbf{B} = \mathbf{0}$ ; thus, based on (10), the corresponding optimization problem becomes

$$\begin{aligned} \max_{\mathbf{A}} \quad & \sum_{n \in \mathcal{N}} \ln \left( \sum_{i \in \mathcal{I}} a_{i,n} r_{i,n}^{(\text{RF})} \right) \\ \text{s.t.} \quad & C_1 : \|\alpha_{i*}\|_1 \leq 1, \forall i \in \mathcal{I} \\ & C_2 : \max\{\alpha_{*n}\} = \|\alpha_{*n}\|_1, \forall n \in \mathcal{N} \\ & C_3 : 0 \leq \alpha_{i,n} \leq 1, \forall i \in \mathcal{I}, \forall n \in \mathcal{N} \end{aligned}, \quad (11)$$

where  $\|\alpha\|_1$  is the norm 1 of the vector  $\alpha$ . Note that in case a given mobile user  $n \in \mathcal{N}$  is not in range, or does not receive any communication resource from  $i$ , the corresponding resource allocation coefficient  $a_{i,n} = 0$ . The constraint  $C_1$  in (11) is related to the use of OMA schemes in the RF wireless system and states that the sum of resources allocated to the mobile users in the service area cannot exceed the size of the pool available in RRU with index  $i \in \mathcal{I}$ . The second constraint ensures us that in every column  $n$ , there will be only one non-negative element or, equivalently, that every user should be able to receive resources from only one RRU.

2) *Standalone VLC-only network*: We have also mentioned that for a standalone VLC network,  $\mathbf{A} = \mathbf{0}$  holds; thus, with respect to (10), the optimization problem can be presented as

$$\begin{aligned} \max_{\mathbf{B}} \quad & \sum_{n \in \mathcal{N}} \ln \left( \sum_{j \in \mathcal{J}} \beta_{j,n} r_{j,n}^{(\text{VLC})} \right) \\ \text{s.t.} \quad & C_1 : \|\beta_{j*}\|_1 \leq 1, \forall j \in \mathcal{J} \\ & C_2 : \max\{\beta_{*n}\} = \|\beta_{*n}\|_1, \forall n \in \mathcal{N} \\ & C_3 : 0 \leq \beta_{j,n} \leq 1, \forall j \in \mathcal{J}, \forall n \in \mathcal{N} \end{aligned}, \quad (12)$$

where the constraints in (12) are the same as in (11), but now they refer to the ROUs and their resources (instead of RRUs).

3) *Hybrid RF-VLC network with selection*: The behavior of scheduling weights in a selection network has also been explained; thus, the problem here takes the most general form

$$\begin{aligned} \max_{\mathbf{A}, \mathbf{B}} \quad & \sum_{n \in \mathcal{N}} \ln \left( \sum_{i \in \mathcal{I}} \alpha_{i,n} r_{i,n}^{(\text{RF})} + \sum_{j \in \mathcal{J}} \beta_{j,n} r_{j,n}^{(\text{VLC})} \right) \\ \text{s.t.} \quad & (11).C_1, (12).C_1, (11).C_3, (12).C_3, \\ & C_3 : \max\{\{\alpha_{*n}^T \beta_{*n}^T\}\} = \|\alpha_{*n}^T \beta_{*n}^T\|_1, \forall n \in \mathcal{N} \end{aligned} \quad (13)$$

where  $C_1, C_2, C_4$  has been already explained. In  $C_3$ , we secure that there is only one non-negative element in a row vector where both columns  $\alpha_{*n}$  and  $\beta_{*n}$  are included, which basically ensures that a user  $n$  is able to receive data from only one RU (RRU or ROU).

4) *Hybrid RF-VLC network with aggregation*: Taking (10) into consideration, the corresponding optimization problem in this new situation can be formulated as

$$\begin{aligned} \max_{\mathbf{A}, \mathbf{B}} \quad & \sum_{n \in \mathcal{N}} \ln \left( \sum_{i \in \mathcal{I}} \alpha_{i,n} r_{i,n}^{(\text{RF})} + \sum_{j \in \mathcal{J}} \beta_{j,n} r_{j,n}^{(\text{VLC})} \right) \\ \text{s.t.} \quad & (11).C_1, (12).C_1, (11).C_3, (12).C_3 \end{aligned} \quad (14)$$

where all the constraints has been analyzed previously, and we observe that there is no restrictions in the number of RUs that a user can connect; thus, it could be both RRUs and ROUs.

We note that the  $\ln(x)$  is a concave function on  $x$ , and that all the arguments that are passed in the objective function (10) are linear with respect to the independent variables (*i.e.*, the scheduling weights  $\alpha_{i,n}$  and  $\beta_{j,n}$ ). Thus, the presented optimization problem can be classified as convex, and the optimal solution is the global maximum of the sum proportional fairness utility function of the RF-VLC system.

#### IV. SIMULATION RESULTS

##### A. Simulation parameters of the wireless access links

Two different formulas are used to model the propagation of wireless signals in both RF and VLC frequency bands.

1) *RF channel model*: The path loss formula that is used here is the one that 3GPP recommends for modeling the propagation of 5G signals in an indoor office scenario [15], *i.e.*,  $L[\text{dB}] = 32.4 + 17.3 \log_{10}(d) + 20 \log_{10}(f_c) + X_\sigma$  where  $d$  [m] is the distance between transmitter (RRU) and receiver (user terminal),  $f_c$  [GHz] is the central carrier frequency, and  $X_\sigma$  is a log-normal random variable – with standard deviation  $\sigma$  – that models the shadow fading.

The multipath fading channel gain is then given by [14],  $g = \sqrt{\frac{K}{K+1}} e^{j\theta} + \sqrt{\frac{1}{K+1}} X_1$ , where  $X_1$  is a complex Gaussian random variable with zero mean and unit variance,  $\theta$  is the phase angle of the Line-of-Sight (LOS) component, and  $K$  is the Ricean  $K$ -factor that verifies  $K = 1$  for distances below the breakpoint distance  $d_{\text{bp}}$ , and  $K = 0$  for  $d \geq d_{\text{bp}}$ .

2) *VLC channel model*: The LoS link from ROU  $j$  to mobile user  $n$ , which is given by the straight line that connects the transmitter-receiver pair under consideration, represents the dominant propagation mechanism in our VLC system [16].

TABLE I: Simulation Parameters of the hybrid RF-VLC system.

$p_o$	1 W	$n_c$	1.5
$\eta$	0.53 A/W	$\Phi_{1/2}$	45°
$\sigma_n^2$	$5 \times 10^{-22} \text{ A}^2$	$d_{\text{bp}}$	5 m
$W$	25 MHz	$P_{\text{rf}}$	1 W
$A_{\text{pd}}$	1 cm <sup>2</sup>	$B$	100 MHz
$T_f$	1	$N_0$	$4.002 \times 10^{-21} \text{ A}^2/\text{W}$
$z$	1.5 m	$f_c$	3.5 GHz

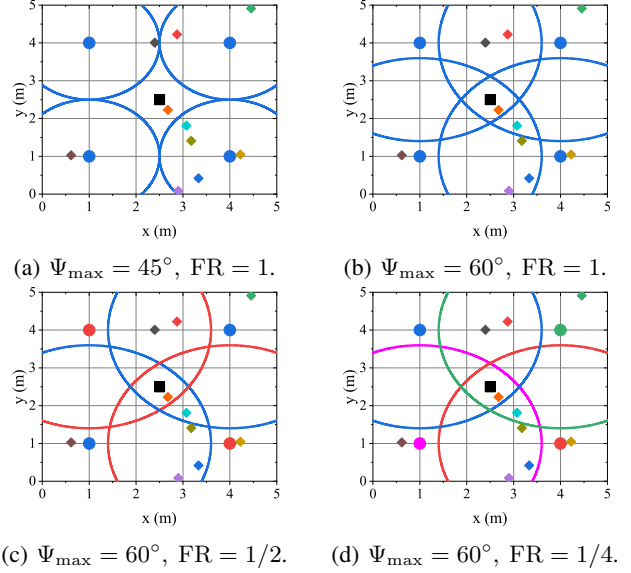


Fig. 2: Layout of the multi-cell VLC system, where colors represent a different portion of orthogonal communication resources for VLC.

Due to that, Non-Line-of-Sight (NLOS) propagation can be neglected since the strength of reflected signals are much weaker than LoS signals in VLC bands [17], [18], [19]. In this situation, the channel power gain is given by [16], [20]

$$h_{j,n} = \frac{(m+1)A_{\text{pd}}}{2\pi d_{j,n}^2} \cos^m(\phi_{j,n}) T_f g_c(\psi_{j,n}) \cos(\psi_{j,n}), \quad (15)$$

where  $d_{j,n}$ ,  $\phi_{j,n}$ , and  $\psi_{j,n}$  are the Euclidean distance, angle of irradiance, and angle of incidence of the VLC link between ROU  $j$  and user  $n$ , respectively. Moreover, we assume that  $m = -\frac{\ln(2)}{\ln(\cos \Phi_{1/2})}$  and  $\Phi_{1/2}$  are the Lambertian emission order and radiation angle at half intensity of the LED, respectively. Similarly,  $A_{\text{pd}}$  is the size of the sensitive area of the PD,  $T_f$  is the transmittance of the optical filter, and  $g_c(\psi_{j,n})$  is the optical concentrator gain [16], [21], *i.e.*,

$$g_c(\psi_{j,n}) = \begin{cases} \frac{n_c^2}{\sin^2(\Psi_{\text{max}})} & 0 \leq \psi_{j,n} \leq \Psi_{\text{max}}, \\ 0 & \psi_{j,n} > \Psi_{\text{max}}, \end{cases} \quad (16)$$

where  $n_c$  denotes the refractive index of the optical concentrator and  $\Psi_{\text{max}}$  is the (semi-angle) of the Field-of-View (FoV) of the PD. Without loss of generality, we assume that all the PDs deployed in the user terminals are pointing up.

3) *Layout of the simulation scenario*: Let  $N = 10$  be the number of randomly deployed users in the target indoor scenario, whereas  $I = 1$  and  $J = 4$  are the number of RRU and ROUs deployed placed at (2.5, 2.5, 1.5) [m] and

(1, 1, 3), (4, 1, 3), (1, 4, 3), and (4, 4, 3) [m], respectively. We assume that the room size is  $5 \times 5 \times 3$  m<sup>3</sup>. The height at which the PDs of the mobile users are placed is assumed constant, *i.e.*,  $z = 1.5$  [m], whereas the corresponding  $(x, y)$  coordinates are assumed random and uniformly distributed over the horizontal plane. The configuration parameters of the hybrid RF-VLC system are summarized in Table I. Note that selected  $f_c$  and  $B$  are aligned with the ones used in 5G scenarios, whereas the values of  $\Psi_{1/2}$  were selected to obtain different overlapping levels among VLC cells. Note that the same electrical modulation bandwidth is used for all the ROUs.

The FoV of a PD is a key parameter to assess the performance of a hybrid RF-VLC system. When the same FoV value is used in all user terminals, different multi-cell scenarios emerge, as illustrated in Fig. 2. In this examples, the solid black squares represent the position of the RRU, whereas the solid circles show the location that the ROUs take in the room. Finally, the rhombuses represent the position that the different randomly deployed users take in a given simulation snapshot. Note that in this image, ROUs that share the same orthogonal resources are shown with the same color (*i.e.*, blue, red, green, and magenta). Note that in Fig. 2a ( $\Psi_{\max} = 45^\circ$ ), there is no overlapping between cells; therefore, no co-channel interference is generated, and only Frequency Reuse (FR) factor 1 is considered (*i.e.*, all ROUs use the same frequency resources). However, in the remaining three configurations that are illustrated in Fig. 2b, Fig. 2c, and Fig. 2d ( $\Psi_{\max} = 60^\circ$ ), some overlapping takes place; due to that, inter-cell interference mitigation is considered and performance of RF-VLC integration approaches is studied when VLC cells use  $FR = 1, 1/2$ , and  $1/4$ , respectively.

### B. Simulation Results and Performance Analysis

Performance analysis has been carried out assuming that  $N = 10$  users are randomly deployed in  $10^6$  independent simulation snapshots. In Fig. 3 we show the Cumulative Distribution Functions (CDFs) of the data rates that each individual user is able to reach in the four different transmission schemes under analysis, which are RF-only, VLC-only, RF-VLC selection, and RF-VLC aggregation. Note that in all these figures, the  $y$ -axis is shown in log-scale to visualize what each configuration provides in the ultra-reliable communications region (*i.e.*, outage probability below  $1 \times 10^{-3}$ ).

When the aim is to maximize the median (or mean) data rate, the most convenient approach is to prevent the existence of co-channel interference in VLC cells with a FR factor as high as possible (black lines,  $\Psi_{\max} = 45^\circ$  and  $FR = 1$ ). This option comes at the cost of a notable outage probability in the case of VLC-only, as about 12% of the indoor area does not have VLC coverage. In contrast, the most convenient option for ultra-reliable communications with VLC-only is to provide full-coverage with overlapping cells, but preventing co-channel interference in VLC using a FR factor as low as possible (green lines,  $\Psi_{\max} = 60^\circ$  and  $FR = 1/4$ ). It should be pointed out that VLC-only (left-hand side figure) does not outperform RF-only (purple lines) in any of the cases

under study, but the integration of RF and VLC using either selection (central figure) or aggregation (right-hand side figure) approaches provides a notable gain when compared to RF-only. This gain is in the order of 50% when studying the median (mean) data rate, and reaches about 100% for data rates at an outage probability of  $1 \times 10^{-5}$  in the case of RF-VLC aggregation. It is important to highlight that the gain of RF-VLC selection with respect to RF-only in ultra-reliable communications regimes is negligible.

In Fig. 4 the  $y$ -axis scale becomes linear, and again we plot the CDFs of the data rates comparing the four different transmission schemes for the same VLC configurations (*i.e.*,  $\Psi_{\max} = 45^\circ$  with  $FR = 1$ ,  $\Psi_{\max} = 60^\circ$  with  $FR = 1$ , and  $\Psi_{\max} = 60^\circ$  and  $FR = 1/2$ ). Their behavior is almost the same as, with respect to the median, the best curves are the aggregated and the selection with small differences, but when it comes to reliability aggregation greatly outperforms every other curve. The interesting part is that RF-only outperforms RF-VLC selection when studying the ultra-reliable communications regime. The performance gains of RF-VLC integration approaches with respect to RF-only are highest in Fig. 4a, then in Fig. 4b, and finally in Fig. 4c. This is because  $\Psi_{\max} = 45^\circ$  with  $FR = 1$  is the VLC configuration in which the benefits of VLC and RF are better complemented (*i.e.*, all VLC cells re-use all bandwidth, no inter-cell interference in VLC cells, and users without VLC coverage are served with RF).

## V. CONCLUSION

Two different approaches were studied in this paper for the integration of RF and VLC resources for indoor wireless access, namely RF-VLC selection and RF-VLC aggregation. In contrast to a VLC-only network, where full-coverage and low inter-cell interference are needed to enable ultra-reliable communications, in hybrid RF-VLC networks it is not necessary to provide full coverage over VLC bands. In these cases, the users located in the cell-center areas of the VLC cells can be offloaded from RF bands, such that these more limited RF resources could be reserved for users that do not have VLC coverage. Although RF-VLC selection and RF-VLC aggregation performed similarly in terms of the median (mean) data rate, the use of RF-VLC aggregation provided a more notable gain with respect to RF-only in the ultra-reliability region of the CDFs. Thus, hybrid RF-VLC networks have the potential to provide a solid solution to the new challenges that B5G indoor scenarios induce, especially when carrier aggregation is used to combine RF and VLC resources.

## ACKNOWLEDGMENT

This publication has been based upon work from COST Action CA19111 NEWFOCUS, supported by COST (European Cooperation in Science and Technology).

## REFERENCES

- [1] H. Holma, A. Toskala, and T. Nakamura, *5G Technology: 3GPP New Radio*. John Wiley & Sons Ltd., 2020.
- [2] E. Dahlman, S. Parkval, and J. Sköld, *5G NR – The next generation of wireless access technology*, 2nd ed. Elsevier, 2021.

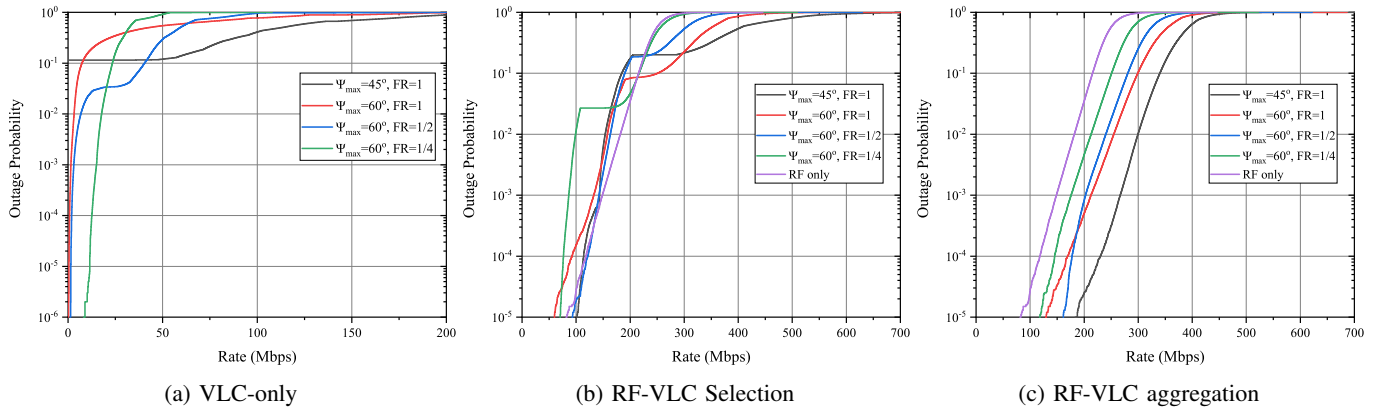


Fig. 3: Effect of the different VLC system configurations (*i.e.*, FoV semi-angles and FR factors) when using different integration approaches for the hybrid RF-VLC system, namely: RF-only, VLC-only, RF-VLC selection, and RF-VLC aggregation.

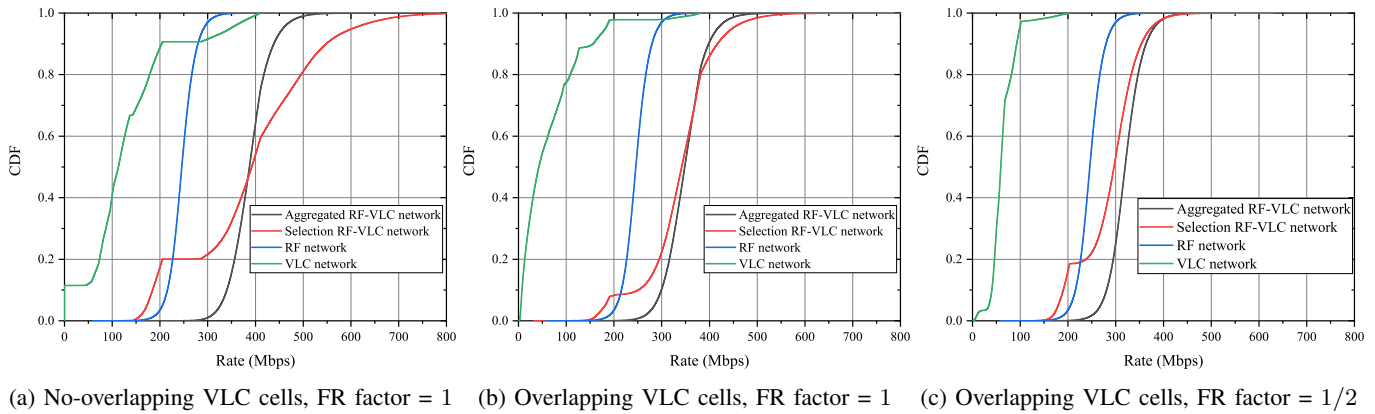


Fig. 4: Effect of the integration approaches on the user data rate in case of different multi-cell VLC configurations. No overlapping ( $\Psi_{\max} = 45^\circ$ ) vs. moderate overlapping ( $\Psi_{\max} = 60^\circ$ ). High FR factor (FR = 1) vs. moderate (FR = 1/2).

[3] W. Saad, M. Bennis, and M. Chen, "A Vision of 6G Wireless Systems: Applications, Trends, Technologies, and Open Research Problems," *IEEE Network*, vol. 34, no. 3, pp. 134–142, May/June 2020.

[4] H. Haas, L. Yin, Y. Wang, and C. Chen, "What is LiFi?" *J. Lightwave Technol.*, vol. 34, no. 6, pp. 1533–1544, Mar. 2016.

[5] B. Genovés Guzmán, A. Dowhuszko, V. Gil Jiménez, and A. Pérez-Neira, "Resource Allocation for Cooperative Transmission in Optical Wireless Cellular Networks With Illumination Requirements," *IEEE Trans. Commun.*, vol. 68, no. 10, pp. 6440–6455, Oct. 2020.

[6] K. Rallis, V. Papanikolaou, P. Diamantoulakis, A. Dowhuszko, J. Hämmäläinen, and G. Karagiannidis, "Design of MAC-layer protocols for distributed NOMA-based VLC networks," in *Proc. Int. Symp. Commun. Syst., Netw. & Digital Signal Process.*, July 2022, pp. 33–37.

[7] V. Papanikolaou, P. Diamantoulakis, P. Sofotasios, S. Muhaidat, and G. Karagiannidis, "On optimal resource allocation for hybrid VLC/RF networks with common backhaul," *IEEE Trans. Cognitive Commun. Netw.*, vol. 6, no. 1, pp. 352–365, Mar. 2020.

[8] M. Abedi, A. Dowhuszko, and R. Wichman, "Visible light communications: A novel indoor network planning approach," in *Proc. IEEE Global Commun. Conf.*, Dec. 2021, pp. 1–7.

[9] A. Dowhuszko and A. I. Pérez-Neira, "Achievable data rate of coordinated multi-point transmission for visible light communications," in *Proc. IEEE Int. Symp. Personal, Indoor, and Mobile Radio Commun.*, Oct. 2017, pp. 1–7.

[10] D. Lee, H. Seo, B. Clerckx, E. Hardouin, D. Mazzaresse, S. Nagata, and K. Sayana, "Coordinated multipoint transmission and reception in LTE-advanced: Deployment scenarios and operational challenges," *IEEE Commun. Mag.*, vol. 50, no. 2, pp. 148–155, Feb. 2012.

[11] F. Ahmed, A. Dowhuszko, and O. Tirkkonen, "Distributed algorithm for downlink resource allocation in multicarrier small cell networks," in *Proc. IEEE Int. Conf. Commun.*, June 2012, pp. 6802–6808.

[12] J.-B. Wang, Q.-S. Hu, J. Wang, M. Chen, and J.-Y. Wang, "Tight Bounds on Channel Capacity for Dimmable Visible Light Communications," *J. Lightwave Technol.*, vol. 31, no. 23, pp. 3771–3779, Dec 2013.

[13] X. Li, R. Zhang, and L. Hanzo, "Cooperative Load Balancing in Hybrid Visible Light Communications and WiFi," *IEEE Transactions on Communications*, vol. 63, pp. 1319 – 1329, 03 2015.

[14] X. Wu, M. Safari, and H. Haas, "Access Point Selection for Hybrid Li-Fi and Wi-Fi Networks," *IEEE Transactions on Communications*, vol. 65, pp. 5375–5385, 2017.

[15] 3GPP. (2018) Study on channel model for frequencies from 0.5 to 100 GHz (3GPP TR 38.901 version 15.0.0 Release 15).

[16] T. Komine and M. Nakagawa, "Fundamental analysis for visible-light communication system using LED lights," *IEEE Transactions on Consumer Electronics*, vol. 50, no. 1, pp. 100–107, 2004.

[17] D. A. Basnayaka and H. Haas, "Design and Analysis of a Hybrid Radio Frequency and Visible Light Communication System," *IEEE Transactions on Communications*, vol. 65, no. 10, pp. 4334–4347, 2017.

[18] M. R. Zenaidi, Z. Rezki, M. Abdallah, K. A. Qaraqe, and M.-S. Alouini, "Achievable Rate-Region of VLC/RF Communications with an Energy Harvesting Relay," in *GLOBECOM 2017 - 2017 IEEE Global Communications Conference*. IEEE Press, 2017, p. 1–7.

[19] H. Kazemi, M. Safari, and H. Haas, "A Wireless Optical Backhaul Solution for Optical Attocell Networks," *IEEE Transactions on Wireless Communications*, vol. PP, pp. 1–1, 12 2018.

[20] H. Ma, L. Lampe, and S. Hranilovic, "Coordinated Broadcasting for Multiuser Indoor Visible Light Communication Systems," *Communications, IEEE Transactions on*, vol. 63, pp. 3313–3324, 09 2015.

[21] J. Kahn and J. Barry, "Wireless infrared communications," *Proceedings of the IEEE*, vol. 85, no. 2, pp. 265–298, 1997.